Transmission-Line Response Using Frequency Techniques

Abstract: Frequency-domain analysis of transmission-line pulse response is presented. A computer program is used to evaluate the response, using subroutines to describe the line characteristics and terminal conditions. The program is applicable to lines of any cross section in which the TEM mode of propagation exists. The line characteristics are obtained from either formula prediction or frequency measurements on small samples. Because of skin effects or complex geometry, these characteristics can be extremely difficult to calculate, and so an experimental procedure is adopted for determining these parameters. The computer-program results are compared to measured values.

Symbols

- A₀ constant term in Fourier series representation
- A_n nth cosine coefficient in Fourier series representation
- B_n nth sine coefficient in Fourier series representation
- $C_{\rm c\,m}$ capacitance per unit length obtained from conformal mapping results
- C_n *n*th value of amplitude and phase spectrum
- I_{ck} current phasor corresponding to cosine coefficient A_k
- I_{sk} current phasor corresponding to sine coefficient B_k
- total length of delay line
- $L_{\rm c\,m}$ inductance per unit length obtained from conformal mapping results
- \mathbf{P}_{ck} transmission line equation coefficient corresponding to cosine coefficient A_k
- $\mathbf{P}_{\bullet k}$ transmission line equation coefficient corresponding to sine coefficient B_k

- Q_{ck} transmission line equation coefficient corresponding to cosine coefficient A_k
- \mathbf{Q}_{sk} transmission line equation coefficient corresponding to sine coefficient \mathbf{B}_k
- R_0 equals $\sqrt{L_{\rm em}/C_{\rm em}}$.
- V_{ek} voltage phasor corresponding to cosine coefficient A_k
- V_{sk} voltage phasor corresponding to sine coefficient B_k
- Z_0 magnitude of characteristic impedance in ohms
- Z_s series impedance due to skin effect
- α attenuation constant in nepers/unit length
- β phase shift in radians/unit length
- γ propagation constant
- δ depth of penetration
- θ_{Z_0} phase angle of the characteristic impedance in radians

Introduction

This paper gives a computer-programmed approach to the analysis of transmission-line propagation using frequency-domain techniques. The characteristics of the transmission line can be predicted by formula, or measured on a small sample, at several frequencies.

Formula prediction is a powerful tool because it can be used to test the feasibility of specific designs, or to vary parameters to determine the effect on the pulse response, or even to try empirical modifications of a formula representation for a given problem to find the most desirable solution. For certain cross-sectional geometries, it may be very difficult (if not impossible) to write a formula describing the transmission line characteristics. For parameter measurement at several frequencies on a small sample, it is possible to predict the pulse response of long lines. The Appendix briefly describes the technique used in this article.

Wigington and Nahman¹ have successfully analyzed the

pulse response of coaxial cables, assuming no dielectric losses and a series skin effect impedance proportional to the square root of the frequency. This analysis can be extended to a limited number of other geometries; however, propagating arbitrary waveforms on transmission lines with arbitrary terminations and varying these terminations to achieve compensating effects due to lossy lines can best be handled using computer techniques.

The line characteristics and terminal conditions are subroutines in the computer program. It is possible to analyze any type of line (e.g., strip or coaxial) and any type of termination merely by inserting the corresponding subroutines. Because of this versatility, the line characteristics can be given in terms of a formula or in graphic form.

The input waveform can easily be described to the computer; any waveform of engineering interest may be used and the response anywhere on the line calculated. The waveform is described by coordinate points which need *not* be equally spaced in time. In the machine computation a straight line is assumed to exist between points.

The paper begins with a general outline of the computer program, followed by a description of the operation of the program. A brief section is included on the mathematical background describing the decomposition into Fourier series, the calculation of the transmission-line equation coefficients in the frequency domain, and the reassembly of the harmonics modified by the line. Also, a formula which has been used successfully to predict pulse response in unsymmetrical strip lines is discussed. The calculated pulse response is compared to the measured pulse response for line characteristics obtained from the unsymmetrical strip line formula and from frequency measurements on a small sample. Also, line characteristics calculated from a strip line formula are compared to measured characteristics using a frequency technique described in the Appendix.

Computer program

The program can be divided into four parts:

- 1) Fourier decomposition of the input waveform.
- Generation of transmission line characteristics, and load and generator impedances, as a function of frequency.
- 3) Solving for the phasor voltages and currents on the transmission line at the point of observation.
- 4) Construction of the output as a function of time by reassembling the harmonics in the time domain.

Any waveform of practical value in electrical engineering can be presented as input data [f(t)] of Fig. 1]. Part MI (Fig. 1) of the program will analyze the waveforms and print out the coefficients of the sine and cosine terms, the amplitude spectrum and the phase spectrum. By selecting

the proper option, it is possible to reconstruct the input waveform using the number of harmonics requested, to see how well the waveform was approximated.

In order to determine the effect of the transmission line on each frequency, the program begins execution of the block of instructions called M2. This block calls upon subroutine SI for the evaluation of α , β , Z_0 , and θ_{Z_0} , using the SI input data, and upon subroutine S2 for the evaluation of terminal conditions and upon the input tape for the total length of the line and the point of observation. The program then executes the instructions in block M3 to get the output. At this point, the programmer has the option of returning to the beginning of block M1 and analyzing another function of time, or of going to block M2 and changing the transmission line description for the same f(t), or of terminating the run.

The computer program is made quite versatile by the use of subroutines for the description of line characteristics and terminal conditions. A subroutine S1 can be written for each type of transmission line. Parameters of each type of line can be changed by varying the input data. A printout of α , β , Z_0 and θ_{Z_0} as a function of frequency is part of the output data, completely characterizing the line in the frequency domain. The author has used two different S1 subroutines: one accepts data in the form of a description of the geometry of the transmission line and calculates the characteristics by formula; the other accepts measured characteristics as points on a log-log graph and interpolates between the points to evaluate these characteristics at the desired frequencies. Subroutine S2 describes the terminal conditions. Here too, the inputs can vary the impedances for any type of termination. Subroutines S1 and S2 can be expressed in formula or in graphical form.*

Special attention has been given to making the program as easy to use as possible by simplifying the description of input quantities. If the whole waveform is approximated by straight lines of arbitrary length, then giving the coordinate points of these lines will describe the input waveform completely.

The inputs to S1 will differ, depending on whether one has a formula or a graphical subroutine. For the formula subroutine pertaining to strip-type lines, the line is easily described on one data card in terms of seven quantities:

- 1) conductor thickness (d)
- 2) conductor width (W)
- 3) permeability of free space (μ_0)
- 4) conductivity (σ)
- 5) inductance/unit length, from conformal mapping results ($L_{\rm c\,m}$)

^{*} There can be more than two subroutines if desired. These subroutines make it possible to solve a wide range of problems involving many different types of lines and terminations.

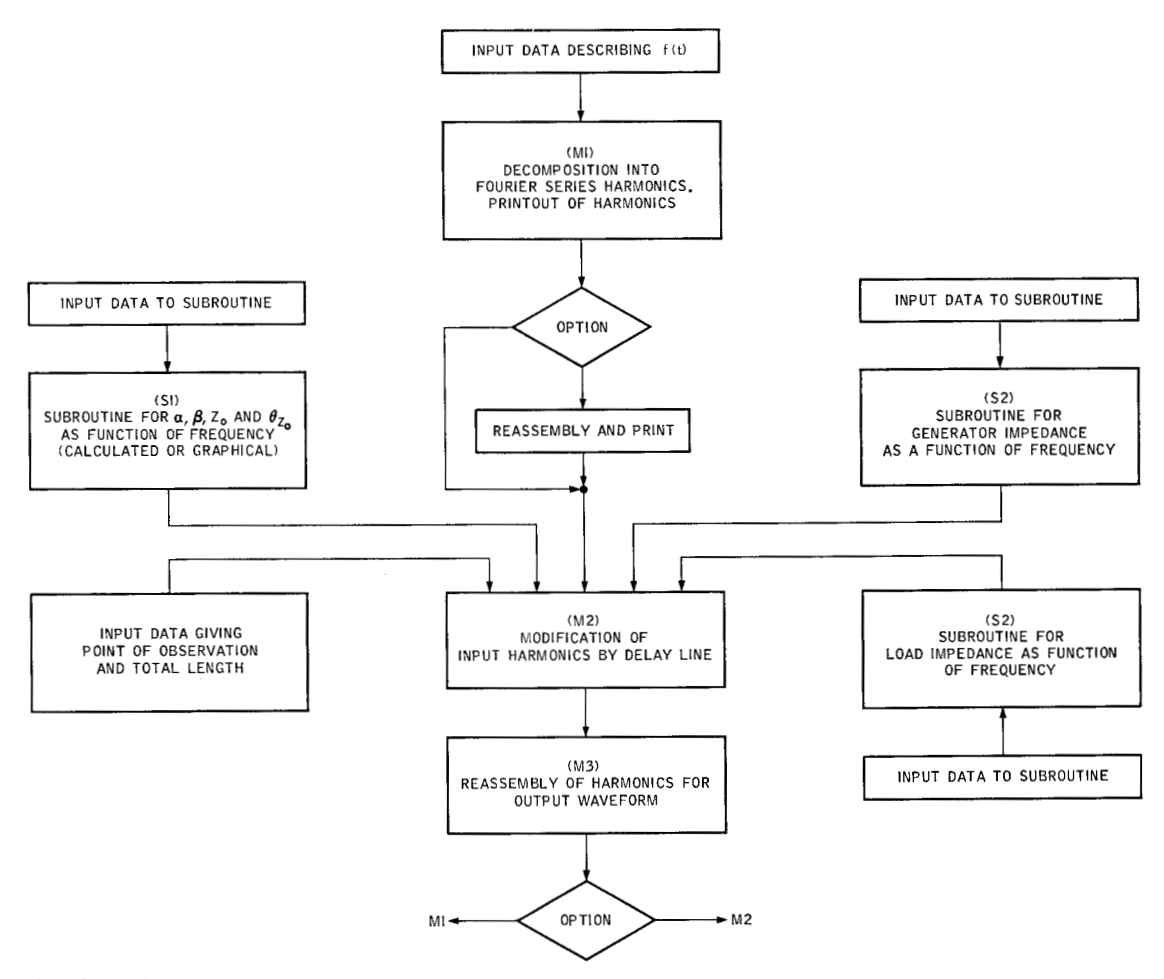


Figure 1 Flow chart of computer program.

- 6) capacitance/unit length, from conformal mapping results ($C_{\rm em}$)
- 7) factor (introduces ground plane series losses as function of W/h ratio)

(Note: d, W, σ and factor are needed to calculate skin effect losses).

When using a graphical description of α , β , Z_0 , and θ_{Z_0} , the same technique as for the description of f(t) of approximating the curve by straight-line segments is used. The curves, however, are assumed to be given on log-log graph paper and the characteristics plotted as a function of frequency.

A parallel *RC* circuit has been assumed adequate to describe terminal impedance conditions. This is easily programmed (subroutine *S2*) with *R* and *C* as the input data. The subroutine may also be written for far more complex terminal impedance conditions.

At this point, a brief example will be given to illustrate the ease with which a problem can be presented to the machine. The formula subroutine is used to describe the line parameters and another formula subroutine to describe the terminal conditions.

The triangular waveform shown in Fig. 2 is applied to the illustrated transmission line. On the first data card is entered the number of harmonics desired, the period of the input f(t), the number of cards to describe the input, and the increment Δt to be used in the final reassembly. The triangular waveform can be described by three sets of coordinates, one set per data card. The total length l and the point of observation x occupy another data card, the cross section (using the formula subroutine SI) takes one more card, and terminal conditions take one card for each end of the line. The total number of cards for the problem is eight.

Mathematical background

• Fourier series decomposition of input waveform

The input waveform f(t) can be expressed as a Fourier series in the following two ways: In terms of sines and cosines,

$$f(t) = \frac{A_0}{2} + \sum_{n=1}^{\infty} A_n \cos \frac{2\pi n}{T} t + \sum_{n=1}^{\infty} B_n \sin \frac{2\pi n}{T} t,$$
(1)

where

$$A_0 = \frac{2}{T} \int_0^T f(t) dt \tag{2}$$

$$A_n = \frac{2}{T} \int_0^T f(t) \cos \frac{2\pi n}{T} t \ dt \qquad (n > 0)$$
 (3)

$$B_n = \frac{2}{T} \int_0^T f(t) \sin \frac{2\pi n}{T} t dt \qquad (n > 0)$$

(n is an integer) (4)

or, in terms of exponentials,

$$f(t) = \sum_{n=-\infty}^{\infty} \mathbf{C}_n e^{j2\pi nt/T}.$$
 (5)

The relationships between Eqs. (5) and (1) are:

for
$$n = 0$$
, $C_0 = A_0/2$

for
$$n > 0$$
 $C_n = \frac{A_n - jB_n}{2}$
$$= \frac{1}{2} \sqrt{A_n^2 + B_n^2 / - \tan^{-1} B_n / A_n}$$

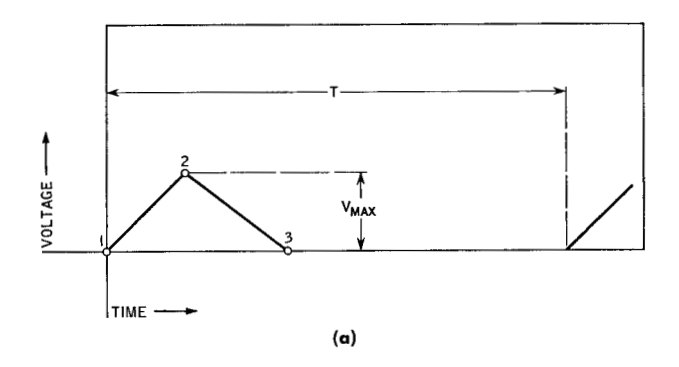
and
$$C_{-n} = \frac{A_n + B_n}{2} = \frac{1}{2} \sqrt{A_n^2 + B_n^2 / \tan^{-1}} B_n / A_n$$
.

The integrals in Eqs. (2), (3), and (4) can be evaluated between time t_1 and t_2 if one assumes that the voltage changes linearly between the two points. The contribution of any straight-line segment to the coefficient may then be calculated by substituting the coordinates of its two end points in the integrated equation. By approximating a given curve by a series of broken lines, one may obtain the Fourier series coefficients by summing the contribution over all segments.

By programming the integrated equation for a typical segment, one can approximate any curve by straight-line segments of any length merely by giving coordinate points as input data and summing over the contribution of each segment.

◆ Transmission line equations

In order to program the transmission-line equations, they must be rewritten in terms of real and imaginary parts; this has been done for all the equations. Once the propagation characteristics α , β , and \mathbf{Z}_0 and the load \mathbf{Z}_L are known as a function of frequency, the input impedance of the line can be calculated for the fundamental frequency and all harmonics from



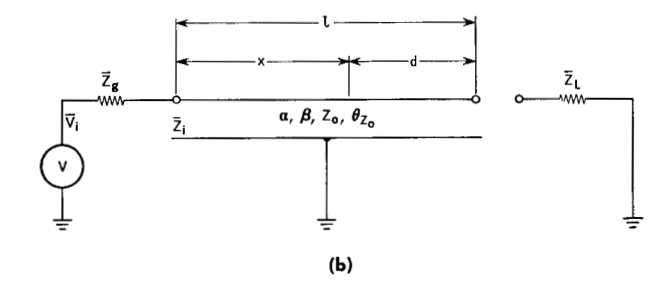


Figure 2 Waveform and line characteristics. Note that μ_0 and σ are known, and $L_{\rm em}$ and $C_{\rm em}$ can be found from conformal mapping results.)

$$\mathbf{Z}_{i} = \mathbf{Z}_{0} \left\{ \frac{1 + \mathbf{k}_{L} e^{-2\gamma l}}{1 - \mathbf{k}_{L} e^{-2\gamma l}} \right\},$$
where $\mathbf{k}_{L} = \frac{\mathbf{Z}_{L} - \mathbf{Z}_{0}}{\mathbf{Z}_{L} + \mathbf{Z}_{0}},$ (6)

and l is shown in Fig. 2. The voltage V in Fig. 2 represents the cosine (or sine) coefficient obtained from Fourier analysis. The voltage

$$\mathbf{V}_i = \frac{\mathbf{Z}_i}{\mathbf{Z}_i + \mathbf{Z}_c} V \tag{7}$$

and is calculated for each frequency, for both sine and cosine coefficients. The values of the transmission equation coefficients **P** and **O** are found from

$$\mathbf{P} = \frac{1}{2} \left(1 + \frac{\mathbf{Z}_0}{\mathbf{Z}_i} \right) \mathbf{V}_i \tag{8}$$

and

$$Q = \frac{1}{2} \left(1 - \frac{Z_0}{Z_i} \right) V_i. \tag{9}$$

The phasor representation of voltage and current at a

particular frequency is given below:

$$\mathbf{V} = \mathbf{P}e^{-\alpha x}e^{-i\beta x} + \mathbf{Q}e^{\alpha x}e^{i\beta x} \tag{10}$$

$$\mathbf{I} = \frac{\mathbf{P}}{\mathbf{Z}_0} e^{-\alpha x} e^{-i\beta x} - \frac{\mathbf{Q}}{\mathbf{Z}_0} e^{\alpha x} e^{i\beta x}. \tag{11}$$

These are the transmission-line equations in phasor form.

• Reassembly of harmonics

After calculating the phasor voltage and current equations for each frequency, one may obtain the outputs as functions of time. Equations (10) and (11) represent phasor equations for a particular frequency and for either cosine or sine coefficients. For the cosine coefficients, one multiplies the phasor equation by $e^{i\omega t}$, takes the real part, and sums it over the fundamental plus all harmonics to get the voltage at time t; for the sine coefficients, one follows the same procedure, except that the imaginary part is used.

As can be seen from the list of symbols, a subscript c refers to a phasor resulting from a cosine coefficient, while s is for one pertaining to the sine; n refers to the particular frequency component (n = 1 is the fundamental; n = 2 is the first harmonic, etc.) Equations (10) and (11) can be rewritten for the kth cosine coefficient as

$$\mathbf{V}_{ck} = \mathbf{P}_{ck} e^{-\alpha_k x} e^{-i\beta_k x} + \mathbf{Q}_{ck} e^{\alpha_k x} e^{i\beta_k x} \tag{12}$$

and

$$\mathbf{I}_{ck} = \frac{\mathbf{P}_{ck}}{\mathbf{Z}_{0k}} e^{-\alpha_k x} e^{-i\beta_k x} - \frac{\mathbf{Q}_{ck}}{\mathbf{Z}_{0k}} e^{\alpha_k x} e^{i\beta_k x}. \tag{13}$$

For kth sine coefficient, they are rewritten as

$$\mathbf{V}_{sk} = \mathbf{P}_{sk} e^{-\alpha_k x} e^{-i\beta_k x} + \mathbf{Q}_{sk} e^{\alpha_k x} e^{i\beta_k x} \tag{14}$$

and

$$\mathbf{I}_{sk} = \frac{\mathbf{P}_{sk}}{\mathbf{Z}_{0k}} e^{-\alpha_k x} e^{-j\beta_k x} - \frac{\mathbf{Q}_{sk}}{\mathbf{Z}_{0k}} e^{\alpha_k x} e^{j\beta_k x}. \tag{15}$$

The voltage and current at the point x can now be resolved as a function of time. The outputs will be due to the contribution of both cosinusoidal and sinusoidal harmonics; thus,

$$v(t) = v_c(t) + v_s(t) \quad \text{and} \tag{16}$$

$$i(t) = i_c(t) + i_s(t) \tag{17}$$

at each time t, and point of observation x, the summation of the contribution of each frequency $(k = 1, 2, \dots, N)$ will result in an output.

The contribution of the cosinusoids to the voltage is

$$v_c(t) = \sum_{k=1}^{N} \left\{ P_{ck} e^{-\alpha_k x} \cos \left(k \omega_1 t - \beta_k x + \theta_{P_{ck}} \right) + Q_{ck} e^{\alpha_k x} \cos \left(k \omega_1 t + \beta_k x + \theta_{Q_{ck}} \right) \right\}. \tag{18}$$

The contribution of the sinusoids to the voltage is

$$v_{s}(t) = \sum_{k=1}^{N} \{ P_{sk} e^{-\alpha_{k}x} \sin (k\omega_{1}t - \beta_{k}x + \theta_{Ps}) + Q_{sk} e^{\alpha_{k}x} \sin (k\omega_{1}t + \beta_{k}x + \theta_{Qs_{k}}) \}.$$
 (19)

Similarly, the currents are found to be:

$$i_{c}(t) = \sum_{k=1}^{N} \left\{ \frac{P_{ck}}{Z_{0_{k}}} e^{-\alpha_{k}x} \right\}$$

$$\cos \left(k\omega_{1}t - \beta_{k}x + \left[\theta_{P_{ck}} - \theta_{Z_{0_{k}}} \right] \right)$$

$$- \frac{Q_{ck}}{Z_{0}} e^{+\alpha_{k}x} \cos \left(k\omega_{1}t + \beta_{k}x + \left[\theta_{Q_{ck}} - \theta_{Z_{0_{k}}} \right] \right) \right\}$$
 (20)

and

$$i_s(t) = \sum_{k=1}^{N} \left\{ \frac{P_{sk}}{Z_{0k}} e^{+\alpha_k x} \sin(k\omega_1 t - \beta_k x + [\theta_{P_{sk}} - \theta_{Z_{0k}}]) \right\}$$

$$-\frac{Q_{sk}}{Z_{0_k}}e^{+\alpha_k x}\sin\left(k\omega_1 t+\beta_k x+\left[\theta_{Q_{sk}}-\theta_{Z_{0_k}}\right]\right)\right\}. \quad (21)$$

The voltage and current waveforms can be found by substituting Eq. (18) and (19) into Eq. (16) and Eqs. (20) and (21) into Eq. (17).

In order to solve the above equations, it is necessary to specify α , β , Z_0 and θ_{Z_0} as a function of frequency. In the computer program this is done by a subroutine which can accept a graphical input, i.e., accept the line parameters from log-log graphical plots, or it can accept a formula input, i.e., calculate the parameters from input data describing the cross-sectional area of the line.

Theoretical prediction of strip-line characteristics

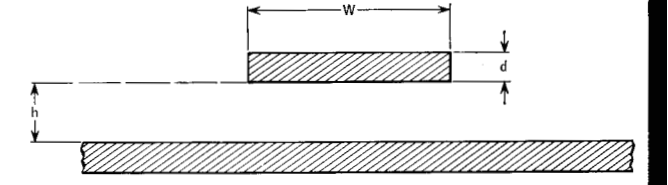
For strip lines (Fig. 3) the formulas for the propagation constant γ and characteristic impedance Z_0 are given by

$$\gamma = \sqrt{(R + jX_L)(j\omega C_{cm})} \tag{22}$$

$$\mathbf{Z}_0 = \sqrt{(R + jX_L)/j\omega C_{cm}} \qquad (G = 0), \tag{23}$$

where the dielectric losses are assumed to be negligible (for epoxy glass this assumption holds into the kilomegacycle range). The capacitance per unit length can be assumed constant over the frequency range; however, the series resistance and inductance vary as a function of frequency because of skin effect.

Figure 3 Strip line cross section.



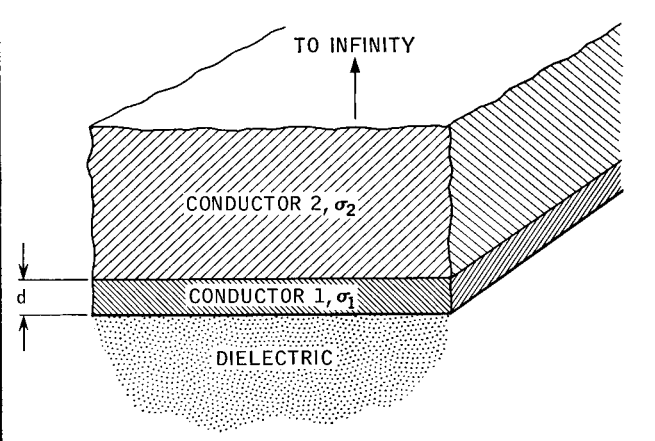


Figure 4 Conductor coating an infinite conductor.

For frequencies where the depth of penetration δ is much smaller than the thickness d, the series impedance due to skin-effect losses can be given by the well-known relationship

$$Z_{s} = \frac{R_{eq}}{W} + j \frac{R_{eq}}{W} , \qquad (24)$$

WITELE

$$R_{eq} = \sqrt{\pi \mu f/\sigma}$$
.

One would like to have a formula which would hold reasonably well over the entire frequency range. As in Ref. 2, we assume (as in Fig. 4) a conductor of infinite thickness with conductivity σ_2 , coated with a conductor having conductivity σ_1 .

Uniform fields are assumed to exist at the surface of Conductor 1. As the conductivity σ_2 goes to zero, Z_s in Conductor 1 can be expressed as

$$Z_s = (1 + j)R_{eg} \coth \tau d \qquad (\sigma = \sigma_1)$$

in ohms per unit length per unit width. For a strip of width W,

$$Z_{\epsilon} = \frac{(1+j)}{W} R_{\epsilon q} \coth \tau d, \qquad (25)$$

where

$$R_{eq} = \sqrt{\frac{\pi f \mu}{\sigma}}$$

$$\delta = \frac{1}{\sqrt{\pi f \mu \sigma}} \tag{26}$$

and

$$\tau = \frac{1+j}{\delta}.\tag{27}$$

The series resistance and reactive impedance due to skin effect can be written as

$$R_{\bullet} = \frac{R_{eq}}{W} \left\{ \frac{\sinh (2d/\delta) + \sin (2d/\delta)}{\cosh (2d/\delta) - \cos (2d/\delta)} \right\}$$
(28)

and

$$X_{s} = \frac{R_{eq}}{W} \left\{ \frac{\sinh (2d/\delta) - \sin (2d/\delta)}{\cosh (2d/\delta) - \cos (2d/\delta)} \right\}. \tag{29}$$

The next step is to examine Eqs. (28) and (29) at high and low frequencies. For high frequencies ($d \gg \delta$), Eqs. (28) and (29) can be written as

$$R_{s} = \frac{R_{eq}}{W} \sqrt{f} = \frac{1}{W} \sqrt{\frac{\pi \mu}{\sigma}} f^{1/2}$$
 (30)

and

$$X_s = \frac{R_{eq}}{W} \sqrt{f} = \frac{1}{W} \sqrt{\frac{\pi \mu}{\sigma}} f^{1/2}.$$
 (31)

These are the same results as those of Eq. (24). For fast-rise-time pulses, Eqs. (30) and (31) are adequate to give the desired response. For low frequencies ($d \ll \delta$), one finds that as f approaches zero,

$$R_s = 1/W\sigma d = \text{dc resistance per unit length}$$
 of the strip

and

$$X_s = 0. (33)$$

These are the results for dc current flow. The value of R in Eqs. (22) and (23) is equal to R_s . The total value of X_L is

$$X_L = \omega L_{cm} + X_s, \tag{34}$$

where the $L_{\rm c\,m}$ term is the inductance per unit length due to the energy stored in the magnetic field between the strip line conductor and the ground plane. The value of $X_s\gg \omega L_{\rm cm}$ for the lower frequencies, but $\omega L_{\rm cm}\gg X_s$ for the higher frequency range. The values of $L_{\rm cm}$ (and also $C_{\rm cm}$) can be found from curves of the results of conformal mappings for static fields due to lossless conductors, because of the similarity between the static field distribution and dynamic distribution at high frequency for lossy conductors.

The formulas giving series resistance and reactive impedance assume that the E and H fields are uniform across the width W of the conductor. This assumption becomes less valid as W/h ratio decreases. Comparing actual responses with calculated responses, one finds that the results are useful down to $W/h \approx 1$. For the high frequencies, the current in the ground plane will not spread out far beyond the width W of the strip line, especially for W/h > 5. Therefore, the series impedance Z_s will be higher than that predicted, and this must be re-

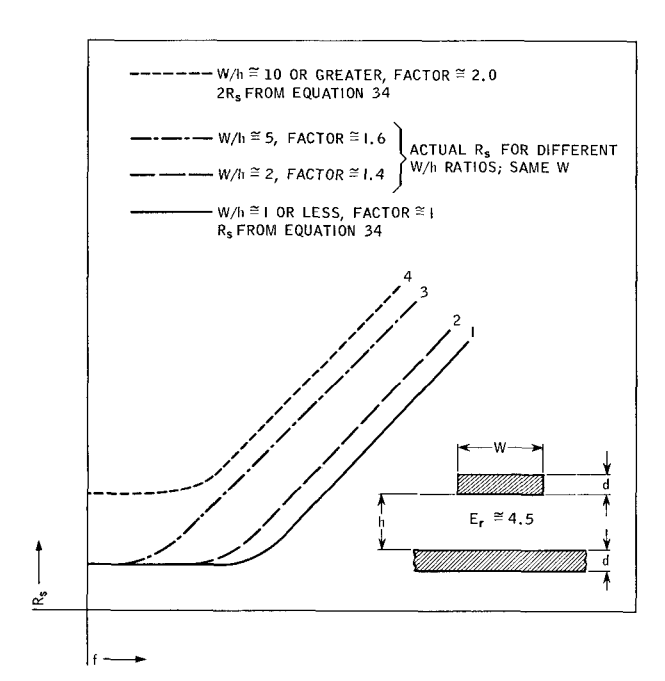


Figure 5 Series resistance plotted vs frequency to illustrate skin effect.

flected in the calculation. A good discussion of ground current spreading can be found in Ref. 3.

Frequency measurements of transmission-line parameters were carried out using the technique given in the Appendix. These will be discussed in detail in the next section. The contribution of the ground plane to the series resistance can best be illustrated by showing the series resistance R_s vs frequency (see Fig. 5). Curves (1) and (4) show the calculated R_s and $2R_s$, respectively, as given by Eq. (28). Curves (2) and (3) show the actual R_s for W/h=2and 5, respectively. Both curves (2) and (3) coincide with (1) for the low frequency range, since the current in a lossy ground plane spreads throughout the plane at low frequencies, so that the resistance is negligible compared to that of the conductor. For high frequencies, the current no longer spreads in the lossy ground plane but concentrates under the strip conductor. In other words, there is a change in the field distribution in going from low to high frequencies (low frequency means $\delta \gg d$, and high frequency means $\delta \ll d$). The current in the plane appears to behave as if at low frequencies the path chosen minimizes the resistance, while for high frequencies the path chosen minimizes the inductance. The degree of concentration at high frequencies varies depending on the W/h ratio; it increases (higher resistance per unit length) for higher W/h ratios. To have formula (28) hold well (especially for high W/h ratio) over the entire frequency range, empirical modification is necessary. However, for most conductor thicknesses, the value of f for

 $\delta=d$ is low enough so that the modification involves only the same constant multiplying factor for all frequencies. [Example: For 1/2 ounce copper at f=13.8 Mc for $d=\delta=0.7$ mil; while for one-ounce copper, and f=3.45 Mc for $\delta=d\cong 1.4$ mils.] This means that for fast-rise-time pulses (150 ns rise time or less, for one-ounce copper) one can select the period of the waveform such that the fundamental harmonic is above the $\delta=d$, so that multiplication by a constant factor between 1.0 and 2.0 in value (depending on W/h) is enough to give a very good approximation. (This will be illustrated in the discussion of Fig. 10).

Results and conclusions

• Comparison of line characteristics vs frequency from formula predictions with measured characteristics

A line was built with the cross section shown in Fig. 6 (W/h ratio of 8.6). Predictions of α , β , Z_0 and θ_{Z_0} were based on this cross-sectional geometry using Eqs. (28) and (29). Because W/h was large, it was supposed that while the series impedance of the top conductor is adequate for the low frequencies, the series impedance rises considerably above the value for a single conductor (at most by a factor of 2) for high frequencies, due to significant concentration of the electromagnetic fields under the conductor.

The values of α , β , etc., were calculated for Z_* and $2(Z_*)$. It was assumed that the measured values would fall between the two limits; for the higher frequencies, the measured curves should approach the theoretical bound established by assuming $2(Z_*)$ as series impedance, and for lower frequencies, they should approach the bound calculated from Z_* as series impedance. The frequency range of the measurements, 100 kc/sec to 30 Mc/sec was chosen since for 1/2 ounce copper, δ becomes equal to the thickness ($d \approx 0.7 \text{ mil}$ of the copper at 13.8 Mc/sec). On either side of this point, one would see the effects of the "low" and "high" frequencies.

Figure 6a shows the calculated curves for R_s and $2R_s$. Measured values of R_s are given using a technique described in the Appendix for measuring the transmission-line characteristics. As can be seen, for low frequencies the resistance values approach the lower boundary corresponding to only the strip conductor loss, while for high frequencies the measured resistance value approaches the curve corresponding to both strip conductor and ground plane losses. Due to the high W/h ratio, the ground-plane losses are just about equal to those of the strip. This implies a change in the field pattern between the strip conductor and the ground plane as the frequency changes from the "low" to the "high" range.

The ground plane, of course, contributes less as the ratio of W/h decreases. It would undoubtedly prove

Figure 6 Comparison of line characteristics vs frequency: calculated parameters vs experimental data. In all cases the calculations were made with series impedance/inch equal to Z_8 and $2Z_8$. Δ represents measured point.

Figure 6a Resistance vs frequency.

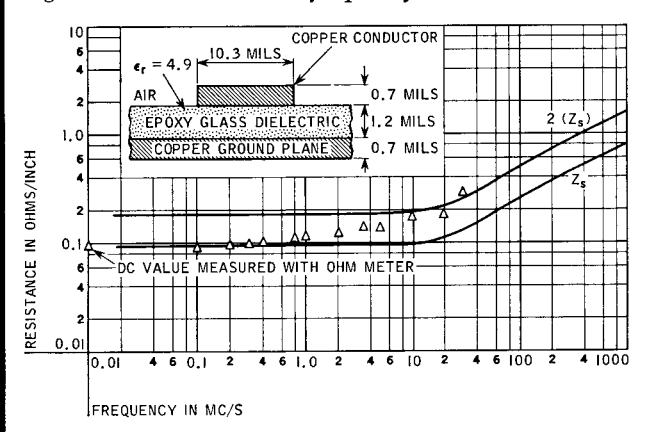
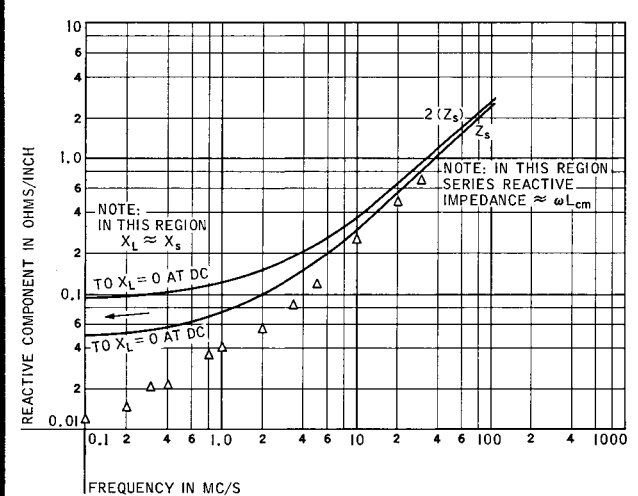


Figure 6b Reactance vs frequency.



useful, as has been previously mentioned, to modify Eqs. (28) and (29) empirically, using measured characteristics, with W/h as a parameter. Another use of the measurement technique would be to measure characteristics of small samples of line as a function of frequency, and then to use these data in the graphical subroutine to predict the behavior of long lines which cannot be built easily (an example of this will be given in a later section).

Both the theoretical calculations and the measured values of the resistance R, the reactance X_L , the attenuation constant α , the phase shift β and the magnitude and

Figure 6c Alpha vs frequency.

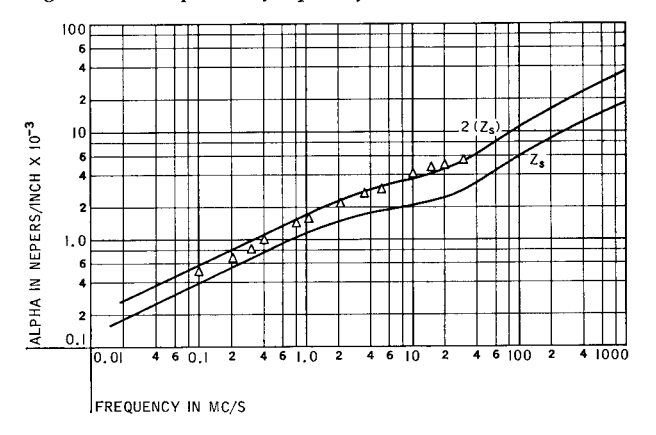


Figure 6d Beta vs frequency.

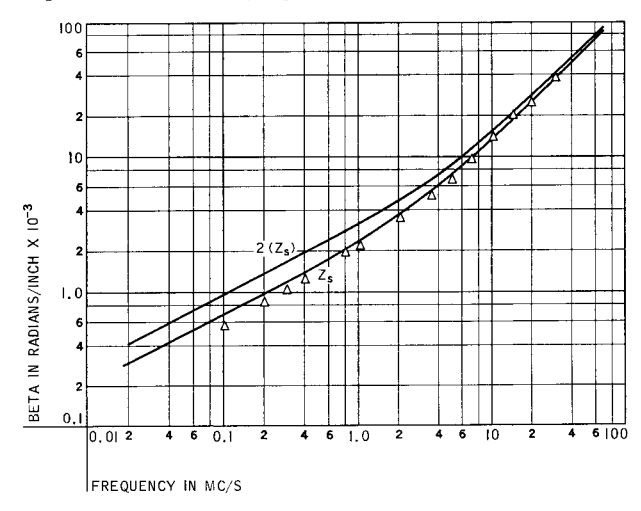
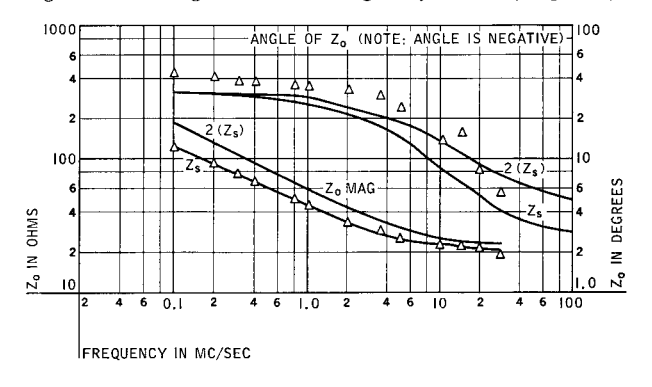
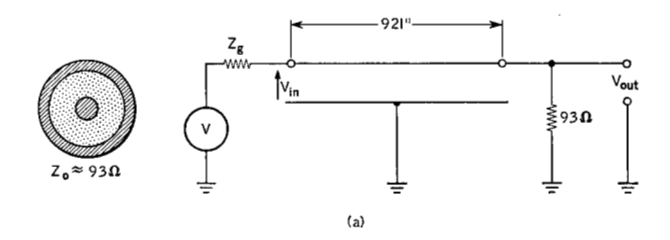


Figure 6e Magnitude and angle of Z_0 vs frequency.



phase angle of the characteristic impedance Z_0 are plotted as a function of frequency (Figs. 6a through e). The value of R series (Fig. 6a) shows good correlation over the entire measured range (dc resistance measurement included)



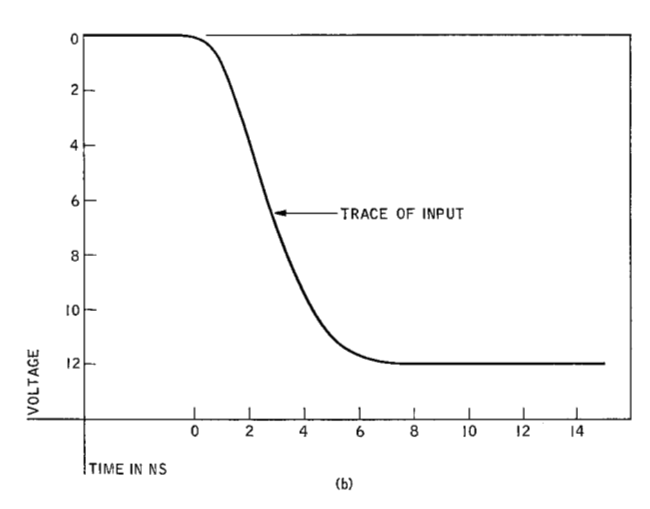


Figure 7 Input waveform to coaxial line. Insert shows transmission line and cross section for coaxial line. The input waveform was simulated using a repeating waveform with the same shaped leading edge.

but X_L (Fig. 6b) correlates well only in the higher frequency range and near the dc value (zero frequency). Since $\omega L_{\rm cm} \gg X_s$ for the high-frequency range, the magnetic fields in the dielectric will contribute virtually all of the series reactance in that range.

Despite the deviation of X_L from the theoretical, the values of α , β , Z_0 and θ_{Z_0} remain close to predicted values over the frequency range shown (Figs. 6b, d and e), although the best correlation is in the higher frequency range.

Prediction of ramp response of long sample from frequency measurements on a small sample

The use of graphical inputs to the computer program in the calculation of pulse response is illustrated here. The points for graphs α , β , Z_0 and θ_{Z_0} were obtained on a small sample of 93-ohm microdot cable, 35 inches long, using the technique described in the Appendix. The impedance-measuring instrument was a Z-g Diagraph. These measurements were checked against the response of a 921-inch sample of the same cable to see whether or not the pulse response could be predicted from frequency measurements on the small sample.

Figure 7a shows the cross section and transmission line.

Figure 7b shows a trace of $v_{\rm in}$. The solid curve in Fig. 8 shows a trace of $v_{\rm out}$. The curve $v_{\rm in}$ was made into the leading edge of a repetitive waveform when formulated for the computer program. The frequency measurements were also given as input data. The points in Fig. 8 show the calculated output and the close agreement.

 Prediction of response to ramp from formula based on line geometry.

Figure 9 shows the cross section, terminating conditions, and point of observation on the transmission line.

A 2-ns-rise-time square wave was used in the program to correspond to the rise time of the waveform used in the test. The results can be seen in Fig. 10. The calculated waveforms for factors of 1 and 1.3 are shown. The use of a factor, whose value varies between 1 and 2 depending on the W/h ratio, was discussed at the end of the section

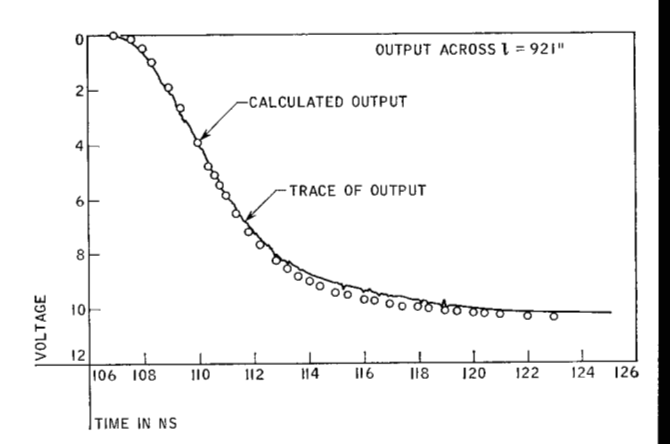
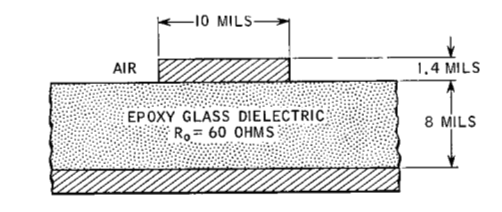
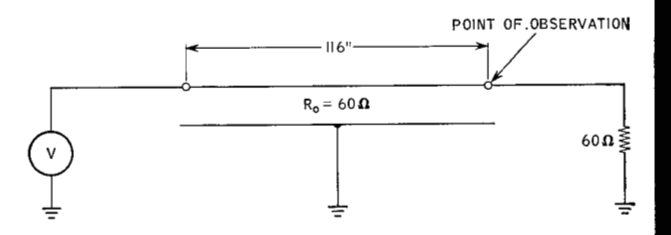


Figure 8 Output voltage across coaxial line.

Figure 9 Cross section and terminal conditions for strip line.





60

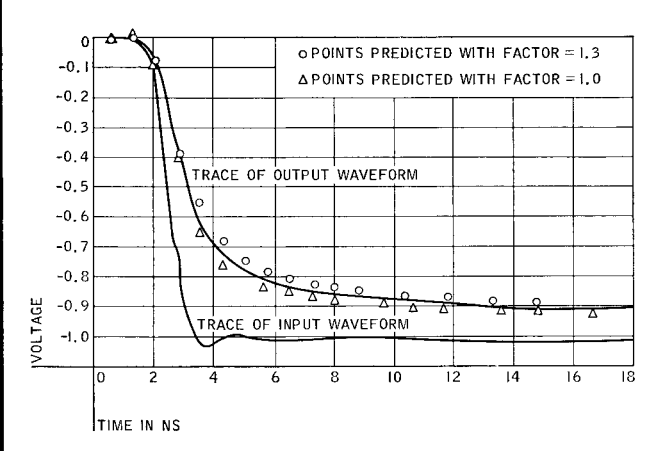


Figure 10 Ramp response of strip transmission line: comparison of theoretical results.

The ramp response was simulated using a repeating waveform with the same shaped leading edge as shown in this Figure.

describing the theoretical prediction of strip line characteristics. A factor of 1 gives an optimistic result, since this means neglecting the ground-plane losses; a factor of 1.3 gives pessimistic results since this exaggerates the ground-plane contribution to the series impedance. In either case, the calculated output is a good approximation to the measured output. A factor of 1.2 will probably give the best approximation.

• Effect of line geometry variations on response

A prediction was made of pulse response on a long, terminated line. Figures 11a and b show the shape of the input waveform, the cross section, terminal conditions, the point of observation and the output waveform. (Note that the input waveform has been shifted down by its dc level since the level is not needed in the solution of the propagation equations). First, the response was computed at the center and at the terminal end of the 22-inch line (Fig. 11a). Next (Fig. 11b), the width of the conductor was maintained as 4 mils, but the conductor was moved closer to the ground plane, thereby decreasing the value of Z_0 , and resulting in a serious deterioration of the waveform. The signal deteriorates from 1 mV (at the beginning of the line) to 0.6 mV in the worse case (for $Z_0 = 20$ ohms).

Summary of results and conclusions

- 1. For large W/h ratios, the field concentrates under the strip line conductor at high frequencies but does not concentrate there at low frequencies. This is due to a change in the field pattern as previously discussed.
- 2. Since the concentration of fields in the ground plane under the strip conductor causes an increase in the

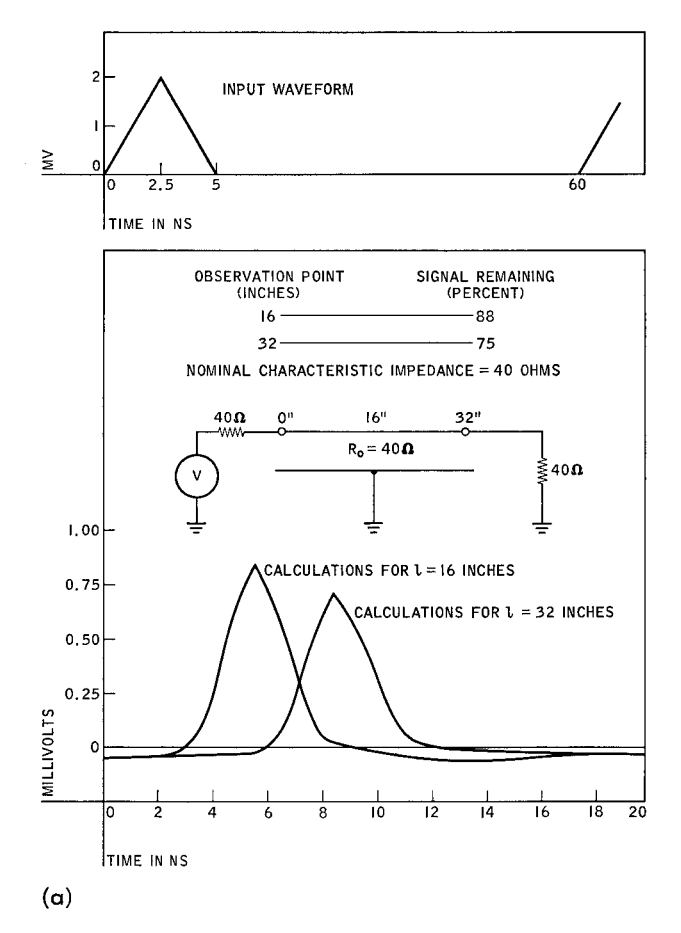
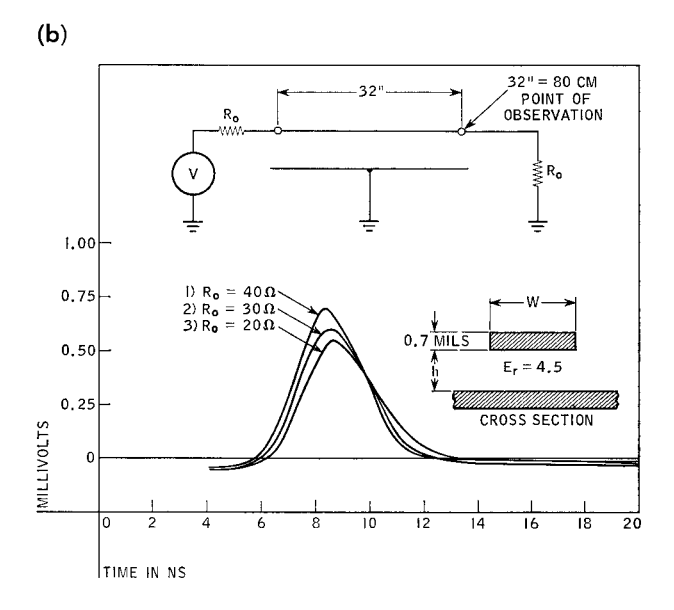


Figure 11 Signal propagation as a function of geometry. (a) Waveform occurring at center of line and at terminating load. (b) Effect of varying h on response at terminating load.

The 2-mV input waveform results in 1 mV on the line at the input. The dc level is rejected in evaluating the output.



series impedance, it would be useful to modify empirically the formula for series impedance using measured data as a function of the W/h ratio. For fast-rise-time pulses, the modification is simply a constant multiplying factor.

- 3. The frequency response measurement of a small sample can be used to predict the response of a transmission line.
- 4. The equation for series impedance used in the formula subroutine gives good results, at least as can be seen from the correlation obtained for the ramp response.
- 5. For the same width of copper (i.e., the same per unit length), pulse transmission suffers serious distortion as the ratio of R/Z_0 increases.

These results show application of the computer program for specific examples. However, the versatility of the program lies in its subroutine for expressing transmission line characteristics and terminal conditions, and in the ease of presenting data to the program. Although the formula subroutine now being used describes the strip-line case, actually any geometry of transmission line can be described if a formula can be derived for it. Using the graphical subroutine permits the characteristics of any line to be measured for a small sample (see Appendix for description of such a technique) and the results applied to a long line with complex terminal conditions. This approach permits the user to go quickly and easily from complex formulas describing the transmission line characteristics in the frequency domain, to time-domain response. The approach also allows the results of empirical modification of transmission line characteristics to be viewed in terms of changes in the time-domain response.

Appendix: Frequency technique for determining transmission-line parameters

Because of skin effects or complex geometry, it may be impossible to calculate transmission-line parameters from a formula. In such cases, the procedure described below can be used to investigate the design of a line by experimental means. This method determines the parameters from open- and short-circuit input impedance measurements on a small sample of line made at several frequencies. The impedance data is processed by an IBM 1620, which generates the characteristic impedance \mathbf{Z}_0 , the resistance per unit length R, the conductance per unit length G, the impedance per unit length L, the capacitance per unit length C, the attenuation constant α , the phase shift β , the phase velocity v_{ϕ} . If the precautions described below are observed in taking the data, the determination of the line parameters becomes a relatively quick and simple operation. The program has been used successfully to evaluate many transmission-line measurements.

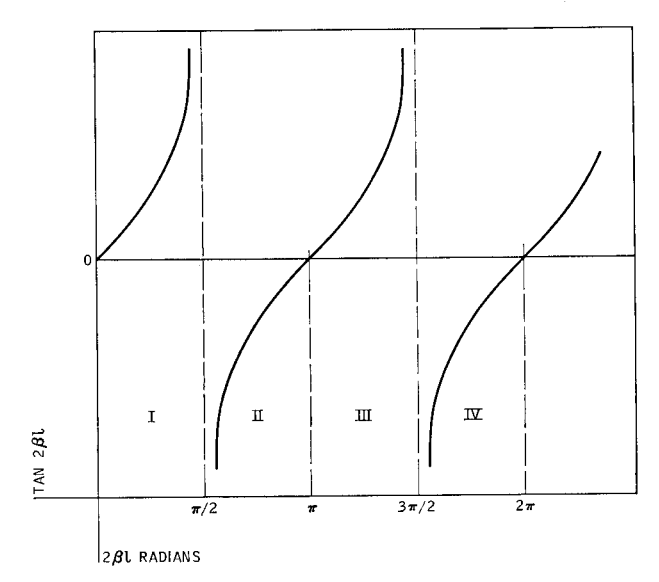


Figure A-1 Behavior of tan $(2\beta I)$.

• Summary of theory

The characteristic impedance of the line is given by

$$\mathbf{Z}_0 = \sqrt{\mathbf{Z}_{sc}\mathbf{Z}_{0c}},\tag{1A}$$

where \mathbf{Z}_{sc} is the short-circuit impedance, and \mathbf{Z}_{0c} is the open-circuit impedance.⁴

The propagation constant is given by

$$\tanh \gamma \mathbf{1} = \sqrt{Z_{sc}/Z_{0c}}.$$
 (2A)

Because the tangent subroutine in the computer does not keep track of quadrants, a problem arises in the computation of β , since the quadrant of tan $(2\beta l)$ must be known for each measurement in order to evaluate the angle $2\beta l$. With the qualification that each new frequency must be higher than the previous frequency, the program keeps track as follows. If the last measurement was in an odd-numbered quadrant, the computer looks for a change in the sign of the difference between the new reading and the old. This means advance one quadrant (Fig. A1). If the previous measurement was in an even numbered quadrant, then a change in the sign of tan $(2\beta l)$ means advance one quadrant. The number of times one goes through all four quadrants is also recorded.

The easiest way to initialize a series of computations is to start in the first quadrant. If the calculated value of tan $(2\beta l)$ is positive, the angle will be calculated in Quadrant I; if negative, the computer will advance to Quadrant II and calculate the angle. In order that the first frequency used be in the first or second quadrant, the criterion is $2\beta l < \pi$. The increment for the change in $2\beta l$ must be less than $\pi/2$, and therefore $\Delta(2\beta l) \cong \pi/2$.

Given l, an approximate value for f can be calculated from

$$eta=2\pi f/v_{\phi}=2\pi f\sqrt{\epsilon_{r}}/C_{\phi}$$
 or $eta=2\pi f\sqrt{LC}$ and so $4\pi f\sqrt{LC}=4\pi f(\sqrt{\epsilon_{r}}l/C_{\phi})<\pi$.

The maximum permissible value of initial frequency is

$$(f_{in})_{\max} = \frac{C_{\phi}}{4l\sqrt{\epsilon_r}} = \frac{1}{4l\sqrt{LC}}$$

and the maximum permissible frequency increment permitted for subsequent calculations becomes

$$(\Delta f)_{\text{max}} = \frac{C_{\phi}}{8l\sqrt{\epsilon_r}} = \frac{1}{8l\sqrt{LC}}$$

If the length of the line sample is such that the lowest frequency of interest is well above $(f_{\rm in})_{\rm max}$, then one may estimate the quadrant and have the program calculate the parameters and print out the quadrant in which the calculation took place. Using this technique, one may find the initializing quadrant and may then proceed.

It is important to note that (especially for lower frequencies) the value of G may be extremely small for a good material and that the inaccuracies of the measured data will not yield accurate values of G (indeed G may

be negative). To get the best results, a few measurements made over a frequency range and plotted on graph paper are desirable because of errors in the experimental set-up. The values of α , β , and Z_0 are not affected nearly as much by experimental errors as are R, G, L, and C because the latter parameters are calculated from the former and cumulative errors are built up.

Acknowledgments

Many thanks are due to Frederick L. Post for his helpful suggestions. The author wishes to thank David B. Eardley for supplying the strip-line pulse response data, Hsung Hsu for supplying the frequency data measured on the 93-ohm microdot sample and Sherman P. Bennett for his help in taking all other data.

References

- R. L. Wigington and N. S. Nahman, "Transient Analysis of Coaxial Cables Considering Skin Effect," *Proceedings of* the IRE 45, 1316 (1957).
- S. Ramo and J. R. Whinnery, Field and Waves in Modern Radio, John Wiley, New York and London, 1953, pp. 249– 252
- H. Cohen, R. Kelisky, and W. Liniger, "Field Spreading in the Ground Plane of a Magnetic Thin Film Memory," IBM Research Report RC-983.
- W. L. Everitt, Communication Engineering, McGraw-Hill, New York, 1937.

Received March 29, 1963